Pflugers Arch - Eur J Physiol (2013) 465:797–804
DOI 10.1007/s00424-012-1184-x

A conserved threonine in the S1–S2 loop of $K_V7.2$ and $K_V7.3$ channels regulates voltage-dependent activation

Yvonne Füll · Guiscard Seebohm · Holger Lerche · Snezana Maljevic

Received: 4 July 2012 / Revised: 2 November 2012 / Accepted: 9 November 2012 / Published online: 28 December 2012

Abstract The voltage-gated potassium channels $K_V7.2$ and $K_V7.3$ (*KCNQ2/3* genes) play an important role in regulating neuronal excitability. More than 50 *KCNQ2/3* mutations have been identified to cause an inherited form of epilepsy in newborns. For two of those (E119G and S122L) found in the S1–S2 region of $K_V7.2$, we previously showed a decreased channel availability mainly at action potential subthreshold voltages caused by a slight depolarizing shift of the activation curve. Interestingly, recent studies revealed that a threonine residue within the S1–S2 loop, highly conserved among different classes of K_V channels, is crucial for both their function and surface expression. To investigate the functional role of the homologous threonine residues in $K_V7.2$ (T114) and $K_V7.3$ (T144) channels, we replaced them with alanine and examined the electrophysiological properties using heterologous expression in CHO cells and whole cell patch clamping. Channels comprising mutant subunits yielded decreased potassium currents with slowed activation and accelerated deactivation kinetics. However, the most striking effect was a depolarizing shift in the voltage dependence of activation reaching +30 mV upon co-expression of both mutant subunits. Potential interactions of T114 within the channel were analyzed by creating a 3D homology model of $K_V7.2$ in an open state suggesting that this residue plays a central role in the formation of a stable interface between the S1–S2 and the S5 segment helices. This could be the explanation why substitution of the conserved threonine in $K_V7.2$ and $K_V7.3$ channels destabilizes the open and favors the closed state of these channels.

Keywords KCNQ2 · Voltage gating · Homology model

Electronic supplementary material The online version of this article (doi:10.1007/s00424-012-1184-x) contains supplementary material, which is available to authorized users.

Y. Füll · H. Lerche · S. Maljevic (✉)
Department of Neurology and Epileptology, Hertie Institute for Clinical Brain Research, University of Tübingen,
Otfried Müller-Str. 27,
72076 Tübingen, Germany
e-mail: snezana.maljevic@uni-tuebingen.de

G. Seebohm
Myocellular Electrophysiology - Institute for Genetics of Heart Diseases (IfGH), Department of Cardiovascular Medicine,
University Hospital Münster,
Münster, Germany

Introduction

Voltage-gated potassium channels (K_V) are activated by membrane depolarization and control the propagation of action potentials and cellular excitability. A functional K_V channel is formed by four subunits assembled into homo- or heterotetramers. The five different isoforms of the K_V7 family encoded by *KCNQ1–5* genes are expressed in the central nervous system ($K_V7.2$–$K_V7.5$), heart ($K_V7.1$) and skeletal ($K_V7.5$) muscle, and in the inner ear ($K_V7.4$). Many mutations affecting *KCNQ* genes, except the *KCNQ5*, have been linked to different inherited diseases [10, 16].

$K_V7.2$ and $K_V7.3$ are major molecular correlates of the neuronal M-current, which can be inhibited by muscarinic receptor agonists. This current regulates the membrane potential at subthreshold voltages and has thereby a strong influence on neuronal firing [2, 3]. Mutations in $K_V7.2$ and $K_V7.3$ can lead to benign familial neonatal seizures (BFNS), an inherited form of epilepsy in newborns. So far, BFNS-causing mutations are found widely distributed within different channel regions (the pore region, the voltage sensor S4, and the C-terminus). They revealed different molecular defects, including changes in ionic conductance, voltage sensing or trafficking, all leading to a reduced M-current and thus hyperexcitable membranes [15].

In $K_V7.2$, two mutations in the S1–S2 loop, S122L and E119G, have been linked to BFNS [9, 24]. Electrophysiological

characterization of these mutations revealed a depolarizing shift of voltage-dependent channel activation and a loss of function restricted to the subthreshold range of an action potential, which demonstrated in human epilepsy the importance of the M-current in this voltage range and indicated that the S1–S2 region is important for channel gating.

McKeown et al. (2008) [18] showed that a highly conserved threonine residue located in the S1–S2 loop of different K_V channels is critical for the surface expression of $K_V1.4$ and $K_V3.1$ channels. They further suggested that this threonine stabilizes the channel via interaction with the outer pore region in the S5–S6 linker. Another study [13] revealed that a small region of S1 interacts with the outer pore helix near the extracellular membrane surface and is necessary for the proper function of different K_V channels. The corresponding threonine was depicted as one of the residues which form the S1–pore interface. Replacement of this residue with an alanine in the Shaker and the $K_V1.2$ yielded no functional channels, but substituting the threonine with serine resulted in the formation of functional channels, emphasizing the importance of a hydroxyl group at this position.

We were interested in the role of this highly conserved threonine at the corresponding positions 114 and 144 in $K_V7.2$ and $K_V7.3$ channels (Fig. 1a). The threonine residues were substituted with alanine and the electrophysiological characteristics of homomeric $K_V7.2$ and heteromeric $K_V7.2/K_V7.3$ channels analyzed in a mammalian cell line. Furthermore, we created a 3D homology model to assess the possible interactions of the threonine residue in the $K_V7.2$ open-state conformation.

Methods

Mutagenesis $K_V7.2$ (NM_004518.4) and $K_V7.3$ (NM_004519.3) cDNAs were kindly provided by Prof. Thomas Jentsch and subcloned into the pcDNA3.1hygro vector (Invitrogen, Darmstadt, Germany). The missense mutation p.T114A (c.A340G) for $K_V7.2$ was inserted using the Quick Change mutagenesis kit (Stratagene, La Jolla, CA, USA). For $K_V7.3$, the p.T144A (c.A430G) mutation was inserted using an overlap PCR strategy with primer pairs carrying the mutation. The PCR product was inserted into the vector via the restriction sites *BamH I* and *Hind III* (Fermentas, St. Leon Rot, Germany) and ligated with T4 DNA ligase (Fermentas, St. Leon Rot, Germany).

Cell culture Chinese Hamster Ovary cells (CHO) were grown in F12 medium (Biochrom AG, Berlin, Germany) supplemented with 10 % fetal calf serum (PAN-Biotech, Aidenbach, Germany) in a humidified incubator at 37 °C with 5 % CO_2. They were passaged two to three times per week. For experiments, cells were plated on 35-mm dishes and transfected using Lipofectamine or Lipofectamine LTX reagent (Invitrogen, Darmstadt, Germany) according to manufacturer's protocol. Cotransfection of cDNA encoding CD8 was used to mark transfected cells using anti-CD8 antibody-coated microbeads (Invitrogen, Darmstadt, Germany). Cotransfections were performed in indicated ratios while the total amount of transfected DNA was kept constant.

Electrophysiology Whole cell recordings of potassium currents in transiently transfected CHO cells were performed at

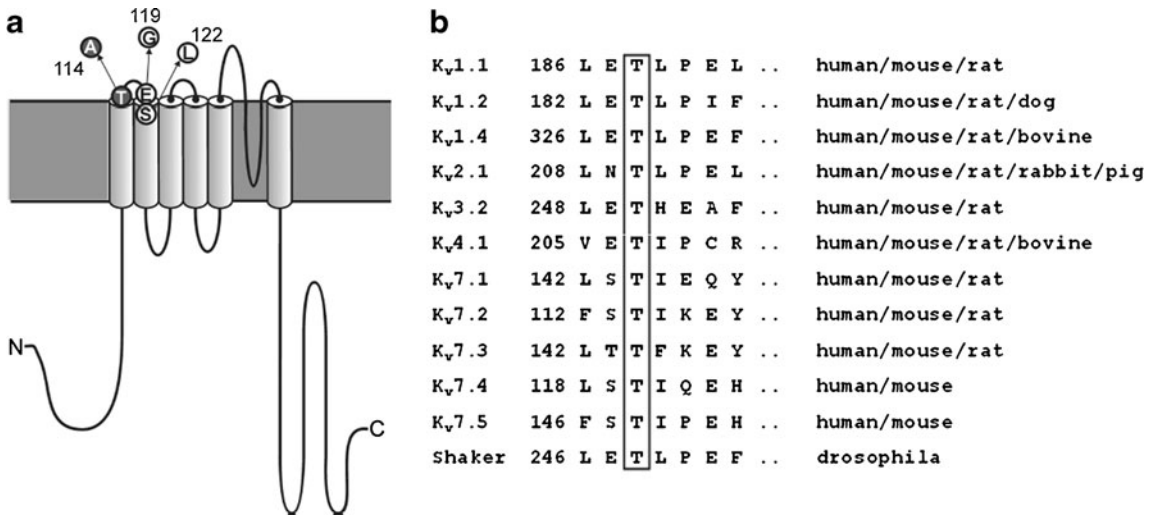

Fig. 1 High conservation of a threonine residue in the S1–S2 loop of different K_V channels. **a** Schematic presentation of the K_V 7.2 subunit presenting the predicted localization of two BFNS-associated mutations, E119G and S122L, and the conserved threonine at position 114, substituted with alanine (T114A) for the functional analysis. **b** Sequence alignment of the S1–S2-loop region of different K_V channels. The threonine residue is highly conserved over species and channels

room temperature (20–22 °C) using an Axopatch 200B amplifier (Axon Instruments, Union City, CA, USA). Data were acquired using pClamp 8.2 software (Axon Instruments) and signals were sampled at 5 kHz and filtered at 2 kHz. Patch pipettes were pulled from thin wall borosilicate glass pipettes with filament (Science Products, Hofheim, Germany) and had a resistance of 1.5 to 3 MΩ. The pipette solution contained (millimolar): 130 KCl, 1 $MgCl_2$, 5 K_2ATP, 5 EGTA, and 10 HEPES adjusted to pH7.4 with KOH. The bath solution consisted of (millimolar): 140 NaCl, 4 KCl, 1.8 $CaCl_2$, 1.2 $MgCl_2$, 11 glucose, and 5.5 HEPES adjusted to pH7.4 with NaOH.

Data analysis Whole cell recordings were analyzed using Clampfit (pClamp, Axon Instruments), Origin 6.1 (OriginLab Corp., Northampton, MA, USA), and Excel (Microsoft, Redmond, WA, USA) software. For recording of potassium currents, standard protocols were used as described before [21]. To quantify current density, the mean value of the steady-state current amplitude recorded at +60 mV was determined for each cell and divided by its cell capacitance. Conductance–voltage curves were derived from tail current amplitudes. The following Boltzman function was fit to the conductance–voltage relationship

$$I\ (V) = I_{\max}/\ (1 + \exp[(V - V_{0.5})/k]) + C$$

with $I_{\max}$ representing the maximum current amplitude at the test potential V, $V_{0.5}$ the half-maximal activation potential, k a slope factor, and C a constant term. Activation kinetics were analyzed using a second-order exponential fit to the current traces, and deactivation kinetics using a first order exponential fit.

All data were shown as mean values±S.E.M. and statistically differences were evaluated by students *t* test and indicated by asterisks with $*p<0.05$, $**p<0.01$, and $***p<0.001$.

Open state model of $K_V7.2$ A consensus $K_V7.2$ model was generated in homology to the refined $K_V1.2$ structure [5]. Several individual modeling steps using the YASARA Structure (version 10.4.11) were undertaken. The model is based on the $K_V7.2$ amino acids 13–324 and refinement of a high-resolution model using a CASP-approved protocol [12]. The PDB database was searched for known structures with a similar sequence using PSI-BLAST [1] to identify potential modeling templates which were ranked based on the alignment score and the structural quality according to WHAT_CHECK [8] obtained from the PDBFinder2 database [7]. $K_V7.2$ models were built for the top scoring template *3LUT*. For each available template, the alignment with the target sequence was iteratively optimized using the evolutionary information contained in related sequences (SwissProt and TrEMBL), the structural information contained in the template, and the predicted target secondary structure [11] used to obtain a structure-based alignment correction (partly based on SSALN scoring matrices) [22]. An indexed version of the PDB was used in order to determine the optimal loop anchor points and to collect possible loop conformations. Insertions, deletions, and dead-end elimination were used to find an initial rotamer solution in the context of a simple repulsive energy function [4]. The loops were optimized and fine-tuning of side-chain rotamers was performed by considering electrostatic, knowledge-based packing, and solvation effects. An unrestrained high-resolution refinement was run using AMBER03. A final hybrid model was built and bad regions in the top scoring model were iteratively replaced with corresponding fragments from the other models.

Results

The position of the conserved threonine residues in a schematic K_V7 channel subunit and the high conservation across K_V channels and species is shown in Fig. 1. The functional consequences of the threonine exchange were analyzed in homomeric $K_V7.2$ as well as in heteromeric $K_V7.2/K_V7.3$ channels, the latter comprising either $K_V7.3$-T144A, or the combination of both threonine mutants. Homomeric $K_V7.3$ channels are claimed to be intrinsically unstable and usually yield no currents in mammalian cell lines or neurons [6], so we could not examine them separately.

Exchange of threonine with alanine reduces $K_V7.2$ currents

Representative current traces of $K_V7.2$-T114A compared to $K_V7.2$ WT channels, as recorded by stepping the membrane potential (Δ10 mV) from the holding potential of −80 to +60 mV for 2 s, are shown in Fig. 2a. They revealed reduced current amplitudes of the mutant. When we compared the current density, calculated by normalizing mean current amplitudes of the last 100 ms of potassium currents recorded at +60 mV to the cell capacitance, mutant channels showed a significant reduction of about 50 % compared to the WT (Fig. 2b).

Threonine substitution in $K_V7.2$ causes a depolarizing shift of voltage-dependent activation, slows activation, and accelerates deactivation

A Boltzman function was fit to the conductance–voltage curves obtained by plotting normalized tail current amplitudes to the voltage of the prepulse to unravel the voltage dependence of channel activation. Mutant $K_V7.2$-T114A channels showed a strong shift in voltage-dependent activation by +25 mV (Fig. 2c, Table 1).

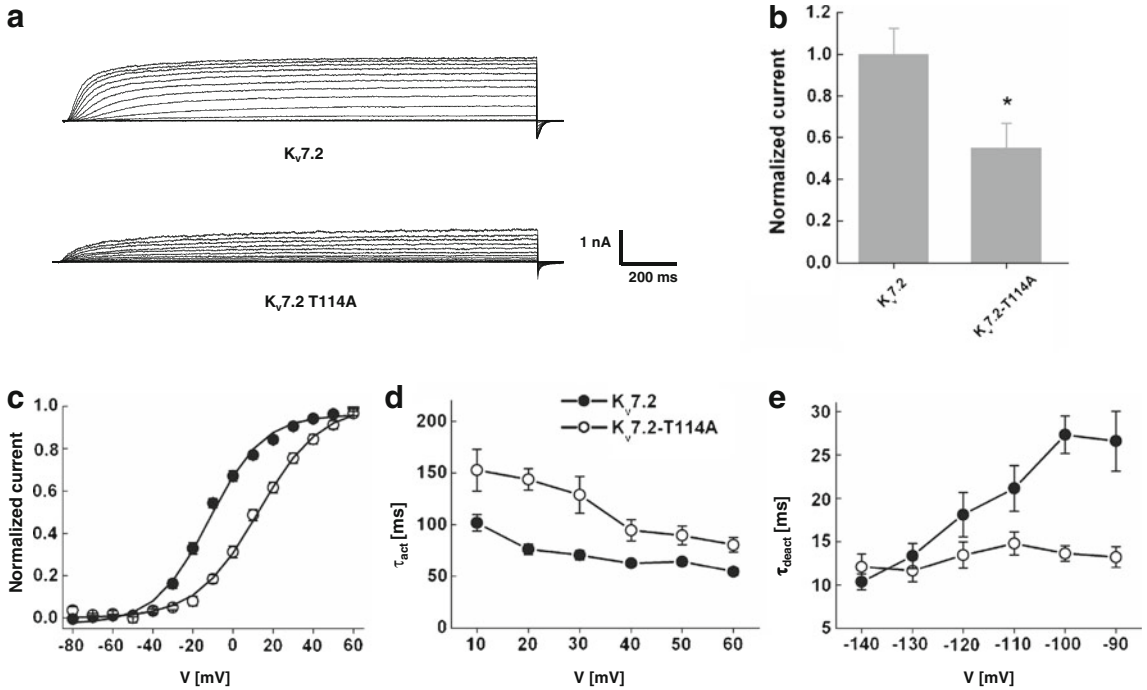

Fig. 2 Electrophysiological properties of the $K_V7.2$-T114A mutation. **a** Representative raw current traces of $K_V7.2$ WT and $K_V7.2$-T114A channels. Currents were elicited from a holding potential of −80 mV by depolarizing steps ranging from −80 to +60 mV in 10-mV steps, followed by a pulse to −120 mV to obtain tail currents. Mutated channels show reduced current amplitudes in comparison to WT, $*p<0.05$. **b** Current densities recorded at +60 mV and normalized to the WT reveal significant reduction for mutant channels. **c** Conductance–voltage curves were constructed by plotting the normalized tail current amplitudes recorded at −120 mV against the membrane potential. Lines represent standard Boltzmann function fitted to the data points. $K_V7.2$-T114A channels show a distinct shift to more depolarized potentials in comparison to WT **d** Time constants of activation (τ_{act}) were obtained by fitting a second-order exponential to the current traces. The faster τ_{act} constant plotted against voltage revealed significantly slowed activation kinetics for the channels comprising $K_V7.2$-T114A. **e** Time constants of deactivation (τ_{deact}) were evaluated by fitting a first order exponential function to the tail current decay at different potentials after a 1.5-s lasting depolarizing pulse to +50. τ_{deact} values plotted against voltage show a reduced voltage dependence so that a significant decrease for $K_V7.2$-T114A is found at −100 and −90 mV. All values are shown in Table 1, n=9–16

To analyze the kinetics of activation, a second-order exponential function was fit to the current traces recorded upon application of 2-s lasting depolarizing voltage steps. In homomeric $K_V7.2$ channels, the mutation leads to pronounced effects on activation kinetics of the channel. Time constants were significantly larger at all potentials between +10 and +60 mV for the channel consisting merely of $K_V7.2$-T114A subunits in comparison to the WT channels (Fig. 2d, Table 1).

The threonine mutation in $K_V7.2$ also leads to a severe impairment of channel deactivation, which was analyzed by fitting a first-order exponential function to the current decay recorded for 0.5 s at potentials between −30 and −140 mV after a 1.5-s prepulse to +50 mV. In homomeric $K_V7.2$-T114A channels, deactivation was up to 2-fold accelerated than in WT channels and revealed almost no voltage dependence (Fig. 2e, Table 1).

Table 1 Electrophysiological properties of homomeric $K_V7.2$ and heteromeric $K_V7.2/K_V7.3$ WT and mutant channels

	$K_v7.2$	$K_v7.2$ T114A	$K_v7.2+K_v7.3$	$K_v7.2+K_v7.3$ T144A	$K_v7.2$ T114A+ $K_v7.3$ T144A
Current density (at +60-mV pulse)	1±0.12	0.55±0.12 *	1±0.17	0.69±0.16 n.s	0.41±0.07**
$V_{0.5}$ [mV], half-maximal activation potential	−12.3±1.3	+12.5±1.3	−11±2	−1.1±1.7	+17.2±1.5
τ_{act} [ms], activation time constant at +20-mV pulse	76±5	144±10 ***	85±8	78±7 n.s.	123±12 *
τ_{deact} [ms], deactivation time constant at −100-mV pulse	27.3±2.2	13.6±0.9 **	33.3±2.2	23.2±3.5 n.s.	11±1.7 ****

All data were shown as mean values±S.E.M.

$*p<0.05$; $**p<0.01$; $***p<0.001$; $****p<0.0001$, statistical differences

Effects of threonine substitution on heteromeric $K_V7.2/7.3$ channel function are similar to the ones observed for $K_V7.2$ homomers

Co-expression experiments with the corresponding mutants of $K_V7.2$-T114A and $K_V7.3$-T144A revealed comparable results. Current density was largely reduced, which was most prominent for the co-expression of both mutant channels (Figs. 3a, b and Table 1). Like homomeric $K_V7.2$-channels, heteromeric channels with $K_V7.3$ also showed a depolarizing shift in voltage-dependent activation when channels with mutated subunits were compared with the WT. Channels comprising both mutant subunits revealed the strongest shift of nearly 30 mV (Fig. 3c, Table 1). Time constants of activation for the heteromeric channels containing $K_V7.3$-T144A and WT $K_V7.2$ subunits were unaltered compared to co-expression of both WT subunits. However, when $K_V7.2$-T114A and $K_V7.3$-T144A subunits were expressed together, the activation time course was significantly slower compared to the WT (Fig. 3d, Table 1). The deactivation time course was significantly accelerated and its voltage dependence decreased when both subunits carried the mutation. This effect was less pronounced and not significant for the $K_V7.3$ mutation expressed with $K_V7.2$ WT (Fig. 3e and Table 1).

Taken together, these observations revealed that channels containing an alanine instead of the conserved threonine residues yield currents with decreased amplitudes, a depolarizing shift in voltage dependence, slower activation, and faster deactivation kinetics.

Discussion

Our study shows that the highly conserved threonine residue in the S1–S2 loop plays an important role for proper $K_V7.2$ and $K_V7.3$ channel functions. When the threonine is substituted with an alanine, we observed reduced current amplitudes, prominent depolarizing shifts in voltage-dependent activation, slowed activation and accelerated deactivation kinetics, all indicating the mutant channels' preference for the closed state conformation.

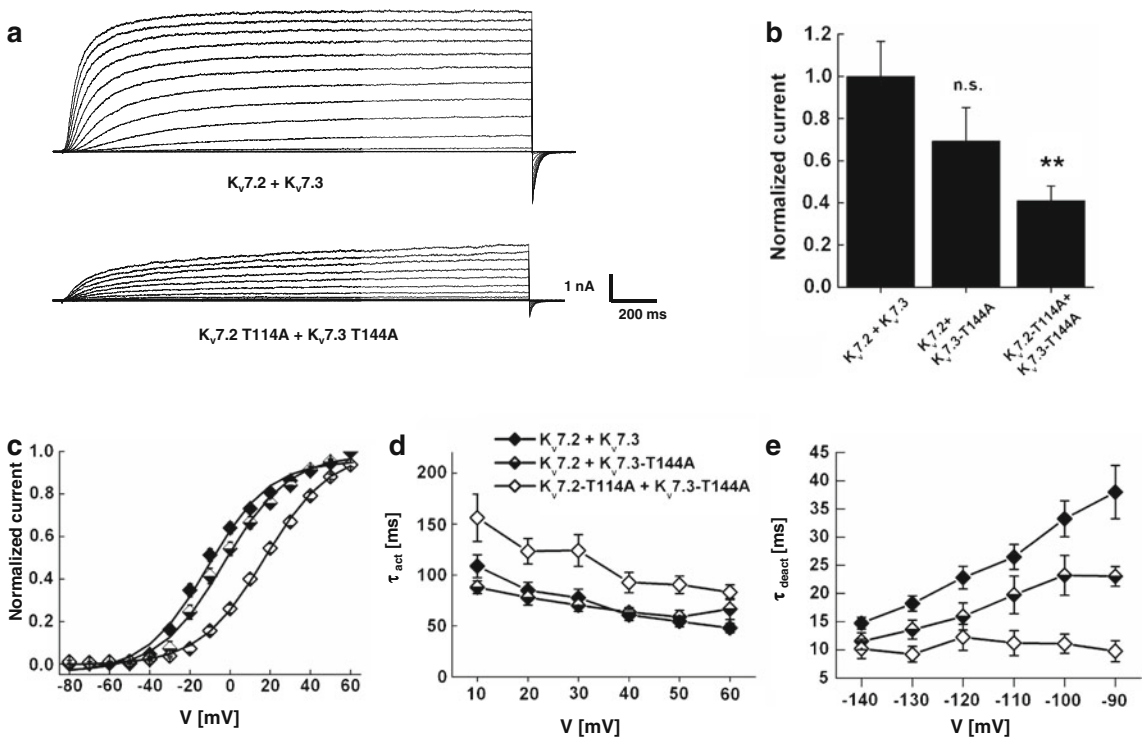

Fig. 3 Electrophysiological properties of heteromeric channels comprising threonine mutations. **a** Representative current traces for $K_V7.2$ and 7.3 heteromeric channels. **b** Normalized current density analyzed at +60 mV decreases for heteromeric channels comprising $K_V7.2$-T114A or $K_V7.3$-T144A. When both subunits are mutated, remaining current is about 40 % of the WT; $*p<0.05$, $**p<0.01$. **c** Coexpression of $K_V7.2$-T114A and $K_V7.3$-T144A causes a strong depolarizing shift in voltage-dependent activation of nearly 30 mV, whereas heteromeric channels composed of WT $K_V7.2$ and mutant $K_V7.3$-T144A subunits show a slight but apparent shift. **d** Fast time constants of activation (τ_{act}) obtained by a second-order exponential fit to the current traces is significantly increased for the $K_V7.2$-T114A+$K_V7.3$-T144A at potentials between +20 and +60 mV. **e** τ_{deact} values plotted against voltage show that heteromeric mutant channels comprising $K_V7.2$-T114A and $K_V7.3$-T144A deactivate significantly faster than the WT at voltages between −140 and −90 mV and show reduced voltage dependence. Coexpression of $K_V7.3$-T144A and $K_V7.2$ reduces τ_{deact} to intermediate values between WT and complete mutant channels. All values shown in the Table 1, $n=9–14$

The importance of the S1–S2 loop and its interaction with the S5 pore loop have been previously proposed for other potassium channels [13] and the conserved threonine at this position has been shown to play a crucial role for the cell surface expression of $K_V1.4$ and $K_V3.1$ channels [18]. The potassium currents of $K_V7.2$ and $K_V7.3$ threonine mutants were reduced, but not completely abolished, suggesting that in contrast to other potassium channels, T114 in $K_V7.2$ and T144 in $K_V7.3$ are not crucial residues regulating the trafficking to the surface. Indeed, our immunostainings of CHO cells transfected with WT or mutant $K_V7.2/K_V7.3$ channels indicated no differences in the expression pattern of the channels (Electronic supplementary material (ESM) Fig. 1). Evenmore, a biotinylation assay revealed no obvious difference in the surface expression of $K_V7.2$ WT and mutant channels (ESM Fig. 2), suggesting that threonine substitution did not cause severe impairment of the channel trafficking.

However, our results show that both threonine residues strongly influence channel gating. In addition to the reduced current amplitudes, we observed prominent effects on the voltage dependence of activation as well as on channel kinetics. When expressed as a homomer, the $K_V7.2$-T114A mutation has a severe effect on both activation and deactivation time constants. In experiments with heteromeric subunits, $K_V7.3$-T144A expressed with WT $K_V7.2$ shows relatively little effects on channel function, whereas channels consisting of mutated $K_V7.2$ and $K_V7.3$ subunits show a comparable dysfunction as four mutated homomeric $K_V7.2$ subunits. Thus, the more mutated subunits, the more pronounced is the effect on channel kinetics. Effects on deactivation were most prominent and included a loss of its voltage dependence.

To get a first idea how these results can be referred to the structural interactions of the channel, we further addressed this issue by 3D-homology modeling and generated an open-state model of the $K_V7.2$ channel (see methods for remarks on the modeling procedure). We find that T114 is involved in the formation of a stable interface between the S1–S2 module and the upper S5 of the pore module. This interface is formed and stabilized by T114 positioned in a crevice built by Y251 and F248 (Fig. 4a). Furthermore, the interface is stabilized by four H bonds, two formed between E119 and K255, the other two between T114 and K255 or Y251 (Fig. 4b). In this model, the side-chain OH of T114 forms H bonds with V111 and the back bone NH of V115. Finally, the back bone NH of T114 builds an H bond with back bone O of F112 (Fig. 4c). The latter bonds allow for stabilization of the S1 interface structure. This S1 surface may attach to the S5 surface stabilized by the described H bonds and additional van der Waals interactions. Mutation of both residues, T114 and E119, may weaken the interaction of the voltage sensor domain with the pore domain. In

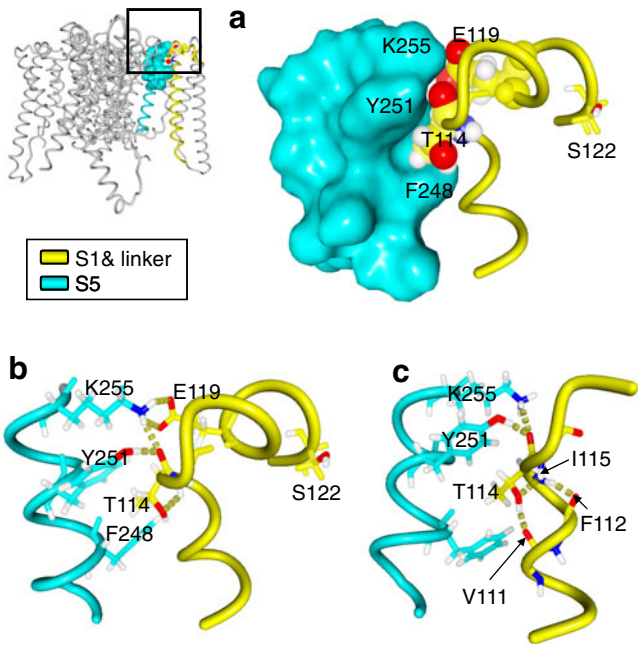

Fig. 4 T114 is positioned in the interface region between the pore and the voltage sensor domain of the $K_V7.2$. An open state model of the transmembrane domains of $K_V7.2$ was generated using a homology modeling approach supported by YASARA Structure 10. An overview of the model is shown above in ribbon representation. The upper S1 and S1–S2 linker and upper S5 are shown in close-up views. **a** The surface of the upper S5 is shown next to the S1/S1–S2 region in ribbon representation. The residues T114 and E119 are shown in space fill representation (CPK *color coded*, C in *back bone color*). K255, Y251, and F248 form a receptor for T114 and E119. **b** Putative H bonds formed between the pore and the voltage sensor domain were computed and are indicated in *yellow*. H bonds between the pore and voltage sensor may stabilize the interaction. **c** T114 is connected to several surrounding residues in a complex hydrogen bonding network that may stabilize the S1/S1–S2 interaction surface

summary, based on our 3D modeling, T114 is located in a central position within the interaction surface of S1/S1–S2 and mutation of this residue can be expected to destabilize the open state and energetically favor channels' closed states.

It has been hypothesized that M-channels have at least four kinetic states, including slow, fast, and intermediate components, with only the intermediate ones showing a voltage dependence [17]. Since our results indicate a decrease in the voltage dependence of the deactivation time constants for mutated channels, which cannot be explained by the observed shift in the open probability curve, the intermediate states may be affected by the mutants and inter-subunit interactions could play an important role for the respective kinetic transitions. In our model, the interaction of the critical threonine residue with the S5 is predicted to occur within the same subunit, so other inter-subunit interactions seem to be important for the observed kinetic effects.

The majority of disease-causing mutations in $K_V7.2$ and $K_V7.3$ is clustered in the pore region and the C-terminus [15] and the S1–S2 channel segment has long time been considered as not being crucial for channel function and even used as a safe spot for a tag insertion [23]. However, detection of two mutations in the S1–S2 loop of the $K_V7.2$ channel that cause neonatal epilepsy indicated that this region is involved in regulating voltage-dependent gating. For both S122L and E119G, we previously reported a depolarizing shift in voltage-dependent activation [9, 24]. Based on these results, on those of previous studies [19, 20] and on the crystal structure of a voltage-gated potassium channel [14], we proposed that an interaction with the voltage sensor S4 might explain these effects [24]. In our new 3D homology model, the residues T114 and E119 seem to be directly involved in important interactions of the S1–S2 region with S5 that stabilize the channel in the open state. The slowed activation and faster deactivation kinetics of channels comprising mutants of these two residues as well as the depolarizing shift in voltage-dependent activation can be referred to the destabilization of the open state, which leads to an energetically favored closed state of the channel. S122 does not appear in this interface and unlike T114A and E119G, the S122L mutation does not affect deactivation kinetics of $K_V7.2$. Thus, S122L may induce a conformational change of the protein region that secondarily affects the S1–S2 interaction with S5, or the functional consequences of this mutant could be underlined by different molecular mechanisms.

In summary, our data reinforce the relevance of the highly conserved threonine residue for voltage-dependent gating of potassium channels, emphasize the role of the S1–S2 loop in these processes and indicate importance of subunit-specific effects and inter-subunit interactions on the function of neuronal K_V7 channels.

Acknowledgments This work was supported by grants from the E-rare program (EUROBFNS, Federal Ministry for Education and Research [BMBF] grant no. 01GM0804 to HL), the European Union (Epicure: LSH 037315 to HL), and the German network for rare diseases of the BMBF (IonNeurONet: 01GM1105A to SM and HL).

References

1. Altschul SF, Madden TL, Schaffer AA, Zhang J, Zhang Z, Miller W, Lipman DJ (1997) Gapped BLAST and PSI-BLAST: a new generation of protein database search programs. Nucleic Acids Res 25:3389–3402
2. Brown DA, Adams PR (1980) Muscarinic suppression of a novel voltage-sensitive K+ current in a vertebrate neurone. Nature 283:673–676
3. Brown DA, Passmore GM (2009) Neural KCNQ (Kv7) channels. Br J Pharmacol 156:1185–1195. doi:10.1111/j.1476-5381.2009.00111.x
4. Canutescu AA, Shelenkov AA, Dunbrack RL Jr (2003) A graph-theory algorithm for rapid protein side-chain prediction. Protein Sci 12:2001–2014. doi:10.1110/ps.03154503
5. Chen X, Wang Q, Ni F, Ma J (2010) Structure of the full-length Shaker potassium channel Kv1.2 by normal-mode-based X-ray crystallographic refinement. Proc Natl Acad Sci U S A 107:11352–11357
6. Gomez-Posada JC, Etxeberria A, Roura-Ferrer M, Areso P, Masin M, Murrell-Lagnado RD, Villarroel A (2010) A pore residue of the KCNQ3 potassium M-channel subunit controls surface expression. J Neurosci 30:9316–9323
7. Hooft RW, Sander C, Scharf M, Vriend G (1996) The PDBFINDER database: a summary of PDB, DSSP and HSSP information with added value. Comput Appl Biosci 12:525–529
8. Hooft RW, Vriend G, Sander C, Abola EE (1996) Errors in protein structures. Nature 381:272. doi:10.1038/381272a0
9. Hunter J, Maljevic S, Shankar A, Siegel A, Weissman B, Holt P, Olson L, Lerche H, Escayg A (2006) Subthreshold changes of voltage-dependent activation of the K(V)7.2 channel in neonatal epilepsy. Neurobiol Dis 24:194–201. doi:10.1016/j.nbd.2006.06.011
10. Jentsch TJ (2000) Neuronal KCNQ potassium channels: physiology and role in disease. Nat Rev Neurosci 1:21–30. doi:10.1038/35036198
11. King RD, Sternberg MJ (1996) Identification and application of the concepts important for accurate and reliable protein secondary structure prediction. Protein Sci 5:2298–2310. doi:10.1002/pro.5560051116
12. Krieger E, Joo K, Lee J, Raman S, Thompson J, Tyka M, Baker D, Karplus K (2009) Improving physical realism, stereochemistry, and side-chain accuracy in homology modeling: four approaches that performed well in CASP8. Proteins 77:114–122. doi:10.1002/prot.22570
13. Lee SY, Banerjee A, MacKinnon R (2009) Two separate interfaces between the voltage sensor and pore are required for the function of voltage-dependent K(+) channels. PLoS biology 7:e47. doi:10.1371/journal.pbio.1000047
14. Long SB, Campbell EB, Mackinnon R (2005) Crystal structure of a mammalian voltage-dependent Shaker family K+ channel. Science 309:897–903
15. Maljevic S, Wuttke TV, Lerche H (2008) Nervous system KV7 disorders: breakdown of a subthreshold brake. J Physiol 586:1791–1801. doi:10.1113/jphysiol.2008.150656
16. Maljevic S, Wuttke TV, Seebohm G, Lerche H (2010) KV7 channelopathies. Pflugers Arch 460:277–288. doi:10.1007/s00424-010-0831-3
17. Marrion NV, Adams PR, Gruner W (1992) Multiple kinetic states underlying macroscopic M-currents in bullfrog sympathetic neurons. Proc Biol Sci 248:207–214. doi:10.1098/rspb.1992.0063
18. McKeown L, Burnham MP, Hodson C, Jones OT (2008) Identification of an evolutionarily conserved extracellular threonine residue critical for surface expression and its potential coupling of adjacent voltage-sensing and gating domains in voltage-gated potassium channels. J Biol Chem 283:30421–30432. doi:10.1074/jbc.M708921200
19. Monks SA, Needleman DJ, Miller C (1999) Helical structure and packing orientation of the S2 segment in the Shaker K+ channel. J Gen Physiol 113:415–423
20. Papazian DM, Shao XM, Seoh SA, Mock AF, Huang Y, Wainstock DH (1995) Electrostatic interactions of S4 voltage sensor in Shaker K+ channel. Neuron 14:1293–1301
21. Peretz A, Degani N, Nachman R, Uziyel Y, Gibor G, Shabat D, Attali B (2005) Meclofenamic acid and diclofenac, novel templates of KCNQ2/Q3 potassium channel openers, depress cortical neuron

activity and exhibit anticonvulsant properties. Mol Pharmacol 67:1053–1066
22. Qiu J, Elber R (2006) SSALN: an alignment algorithm using structure-dependent substitution matrices and gap penalties learned from structurally aligned protein pairs. Proteins 62:881–891. doi:10.1002/prot.20854
23. Schwake M, Pusch M, Kharkovets T, Jentsch TJ (2000) Surface expression and single channel properties of KCNQ2/KCNQ3, M-type K+ channels involved in epilepsy. J Biol Chem 275:13343–13348
24. Wuttke TV, Penzien J, Fauler M, Seebohm G, Lehmann-Horn F, Lerche H, Jurkat-Rott K (2008) Neutralization of a negative charge in the S1–S2 region of the KV7.2 (KCNQ2) channel affects voltage-dependent activation in neonatal epilepsy. J Physiol 586:545–555. doi:10.1113/jphysiol.2007.143826